



Stabilized Exfoliated Black Phosphorus Nanosheets for Fungal DNA-Extraction Assay

Sun Min Lim^{1,2} · Huifang Liu² · Myoung Gyu Kim² · Eun Yeong Lee² · Hyo Joo Lee² · Yeonjeong Roh² · Minju Lee² · Bonhan Koo² · Yong Shin^{1,2} 

Received: 20 May 2024 / Revised: 5 September 2024 / Accepted: 27 September 2024 / Published online: 19 November 2024
© The Korean BioChip Society 2024

Abstract

DNA extraction is essential in fields like medicine, biotechnology, and environmental science. Traditional DNA-extraction methods often face challenges, especially with organisms like *Aspergillus* that have tough cell walls. We propose a novel method using black phosphorus nanosheets (BPNSs) in NMP(1-Methyl-2-pyrrolidinone)–NaOH solvent with dimethyl sulfoxide (DMS) for efficient fungal DNA extraction. BP, with its unique layered structure and photothermal effects, combined with laser irradiation, eliminates thermal steps and hazardous chemicals, simplifying the process. Hence, BPNSs in NMP–NaOH solvent with DMS (BNNDs) are synthesized via a liquid-phase ultrasonic exfoliation method in NMP–NaOH solvent to produce monolayer BP, with the NMP–NaOH serving as the lysis buffer and DMS as the cross-linking agent. This approach significantly improves fungal spore lysis and DNA capture efficiency, achieving fungal DNA isolation in under 15 min with high sensitivity and specificity. Real-time qPCR analysis shows lower threshold cycle values and higher DNA yields compared to commercial kits. This technique is efficient, less labor-intensive, and avoids hazardous chemicals, unlike commercial kits. The assay has high sensitivity, detecting fungal DNA concentrations as low as 10^1 spores per mL. This BNND method offers a rapid, simple, and highly efficient solution for fungal DNA extraction, promising significant advancements in research and diagnostics across various fields.

Keywords *Aspergillus* · Nucleic acid extraction · Black phosphorus nanosheets · Homobifunctional imidoesters · Molecular diagnostics

1 Introduction

Identification of pathogens is crucial in the field of medical diagnostics for accurate detection of infectious diseases and treatment selection [1, 2]. Particularly, fungal pathogens, estimated to comprise around 5 million species, are responsible for over 1.6 million deaths each year from fungal infections [3, 4]. Early diagnosis of these fungal diseases is

significant to prevent progression to life-threatening stages of infection. However, the detection of fungal pathogens is challenging due to the difficulty of distinguishing molds from other types of invasive diseases, the non-specificity of early-stage symptoms, and the absence of a standard test for diagnosis [5, 6]. Common diagnostic tests include skin tests to observe immune responses, body-fluid tests that use tissue or blood for the histologic detection of fungi, and imaging tests, including chest X-rays [7–9]. These diagnostic methods, however, consume a lot of time and are inadequate for clinical use where rapid and accurate diagnosis of infection is crucial.

The polymerase chain reaction (PCR) emerged as a cornerstone for fungal species detection, offering rapid and highly specific direct sample testing [10]. To optimize the efficiency of this PCR technique, it has become essential to extract fungal DNA as extensively as possible, facilitating detection even at minimal levels. However, the resistance of fungal cell walls to traditional DNA-extraction

Sun Min Lim and Huifang Liu contributed equally to this work.

✉ Yong Shin
shinyongno1@yonsei.ac.kr

¹ Life Science and Biotechnology, Underwood International College, Yonsei University, 50 Yonsei-Ro, Seodaemun-Gu, Seoul 03722, Korea

² Department of Biotechnology, College of Life Science and Biotechnology, Yonsei University, 50 Yonsei-Ro, Seodaemun-Gu, Seoul 03722, Korea

protocols posed a bottleneck, leading to inefficient isolation of genomic DNA [11, 12]. Existing DNA-extraction methods using commercial kits often result in poor DNA quality and quantity, and choosing an appropriate protocol remains subjective and dependent on factors like cost and available equipment [13–15]. In addition, while many DNA-isolation protocols are organism-specific, few are optimized for fungal extraction, and commercial alternatives often require multiple steps and specialized tools and reagents [16, 17]. Considering the critical importance of fungal DNA purity and integrity for PCR efficiency, addressing these extraction challenges is crucial for advancing mycology and medical research.

The utilization of nanoparticle composites has emerged as a novel method for nucleic acid detection of viral infectious diseases, showing various advantages in the diagnostics field [18–21]. Recently, we have reported findings where we utilized black phosphorus (BP) for DNA extraction from *Escherichia coli* [22]. BP is a two-dimensional material with a structure of nanosheets stacked over one another [23]. It possesses several advantages, including strong optical absorption, biocompatibility, and a large surface area, making it suitable for diverse biologic applications [24–26]. The study on DNA extraction from *E. coli* by combining BP with laser irradiation demonstrated the possibility of eliminating incubation steps, streamlining the process, and reducing reliance on hazardous chemicals [22]. However, this approach faced limitations due to the instability and non-uniformity of black phosphorus nanosheets (BPNSs) synthesized in distilled water (DW), particularly in its applicability to organisms with complex cell structures, such as fungal species like *Aspergillus*. In addition, BP material is known to undergo degradation under the influence of oxygen and water, causing layers to aggregate and re-form into oxidized phosphorus compounds [27–29].

To address the challenges of conventional DNA-extraction methods, we developed a BPNS in NMP–NaOH solvent with DMS (BNND) method using stabilized BPNSs exfoliated in an organic solvent for efficient DNA extraction from fungal spores, including *Aspergillus*. By leveraging the unique properties of BP, we aimed to overcome existing limitations and establish a rapid and reliable fungal DNA-isolation method. BPNSs were synthesized in organic solvents to create stable and uniformly distributed nanosheets. The BNND-based fungal DNA-extraction method utilizes BPNS material synthesized through liquid-phase ultrasonic exfoliation. This method employs ultrasonic waves to disrupt the weak van der Waals interactions between BP layers, using suitable solvents that prevent degradation. Four organic solvents (NMP, NMP–NaOH, IPA, and DMSO) were tested, with DW included for comparison. These solvents provide stable dispersions of phosphorene, resulting in high BP-flake

yields. We compared BPNSs synthesized in these solvents to select the most efficient material for fungal DNA isolation.

The BNND strategy enriches and extracts fungal DNA in under 15 min. BPNSs in NMP–NaOH solution (BNNs) serve as the lysis buffer, while DMS acts as the cross-linking agent. The technique involves spore lysis, DNA capture, and DNA elution, being efficient, non-labor-intensive, and free of hazardous chemicals compared to commercial kits. This optimized method demonstrates higher DNA-extraction efficiency and effectiveness in detecting *Aspergillus* in spiked milk, suggesting broad applications in diagnostics and food safety. Overall, this BNND-based method offers a simple, rapid, and highly efficient solution for DNA extraction in research and diagnostics.

2 Experiments

2.1 Chemicals and Reagents

All reagents employed were of analytical purity and were utilized without additional purification. 1-Methyl-2-pyrrolidinone (NMP; C_5H_9NO , 99.5%), dimethyl sulfoxide (DMSO; C_2H_6OS , 99.5%), dimethyl suberimidate dihydrochloride (DMS; Sigma, 179523-5G), tris (2-carboxyethyl) phosphine hydrochloride solution ($C_9H_{15}O_6P \cdot HCl$, pH 7.0), Tween 20 (P2287), sodium hydroxide solution (50% in H_2O), and sodium hydroxide pellets (HNaO, 98%) were purchased from Sigma-Aldrich (St. Louis, MO, USA). Isopropyl alcohol (IPA; C_3H_8O , 99.9%) was obtained from Duksan General Science (Seoul, Republic of Korea). Sabouraud dextrose agar with chloramphenicol media (Cat. No. C6781; Lot No. 437412) was obtained from Hardy Laboratories (Santa Maria, CA, USA). 99% ethyl alcohol, DW (UltraPure™, Invitrogen, USA), and phosphate-buffered saline (PBS, 10×, pH 7.4, Thermo Fisher Scientific, Cas No. 12579099) were also used in the experiments.

2.2 Instruments and Kit

A commercial DNA-isolation kit (QIAGEN QIAamp DNA Mini Kit, Cat No. 51304; Maryland, USA) was used for comparing *Aspergillus* DNA-extraction efficiency. A 130-W ultrasonic processor (20kHz, Model no. VCX 130PB, Sonics & Materials Inc., Newtown, CT, USA) was used for liquid exfoliation of BP powders and BNNs synthesis. An 808 nm laser (Beijing Leizhiwei Photoelectric Technology Co., Ltd., China) was irradiated on BNNs to utilize their photothermal characteristics for DNA isolation. A CO_2 incubator (BB 150, Thermo Scientific™, 51023122) was used for *Aspergillus fumigatus* culture. Disposable hemocytometers (C-Chip) were purchased from Incyto (Cheonan, Republic of Korea). A vortex mixer (T5AL, Daihan Scientific Co., Ltd.,

Wonju-Si, Republic of Korea) and a Magic Mixer (TMM-5, Topscien Instrument Co., Ltd., China) were used for thorough mixing of solutions inside the tube. The CFX96 Touch Real-Time PCR Detection System, purchased from Bio-Rad (USA), was used to evaluate DNA-isolation efficiency.

2.3 Biologic Samples

Aspergillus fumigatus (ATCC36607) was used in the present study. It was cultured in Sabouraud dextrose agar medium plates using the center culture method and incubated at 25 °C for 5 days. *A. fumigatus* spores, generated during its growth phase, were harvested using 0.01% Tween 20 Buffer in DW. After thorough washing in PBS through centrifugation (1500 rpm; 3 min), which was repeated three times, the spores were stored in DW for future use in experiments and their concentrations were quantified using light microscopy at 200× magnification in a hemocytometer chamber.

2.4 Preparation of the Black Phosphorus Nanosheets (BPNS)

BP crystals with a purity of 99.999% were purchased from 2D Semiconductors. BPNSs were synthesized using a liquid-phase ultrasonic exfoliation method (Fig. 1a) [30, 31]. In this “top-down” approach for layered BP preparation, BP crystals were initially ground into BP powders. Subsequently, 10 mg of these powders were dispersed in 10 mL of various liquid solvents. Five types of solvent—distilled water (DW), N-methyl-2-pyrrolidone (NMP), NaOH-saturated

NMP (NMP–NaOH), isopropyl alcohol (IPA), and dimethyl sulfoxide (DMSO)—were used in the present study. These solvents were selected based on their common usage and high BP-exfoliation yield [32, 33].

The mixture was subsequently subjected to probe sonication at 20 kHz frequency and 130 W for 8 h. Following sonication, the BP suspensions were centrifuged at 2000 rpm for 10 min to eliminate the unexfoliated bulk material, and the supernatant solutions were further centrifuged at 14,000 rpm for 10 min. The resulting precipitate was then redispersed in DW for further experimental use.

2.5 Characterization of BNNs

A handheld infrared thermal imager (A-20, Test Tools, China) was employed to investigate the photothermal characteristics of BNNs. A field emission scanning electron microscope (FE-SEM; JSM-7500F JEOL) was utilized to characterize the surface morphologies and determine overall uniformity and size of the BP materials. The stability and size distribution of the materials were assessed through zeta potential and dynamic light scattering (DLS) using a Zetasizer NanoSP instrument (Malvern, United Kingdom). Energy dispersive X-Ray (EDX) analysis was used to determine the elemental composition of the BP material, and X-Ray diffraction (XRD; Ultima IV, Rigaku) analysis was used to analyze BNN crystalline structures. In addition, atomic force microscopy (AFM; NX-10, Park Systems) was conducted to obtain information on the topography of BNN materials and the mechanism behind spore lysis.

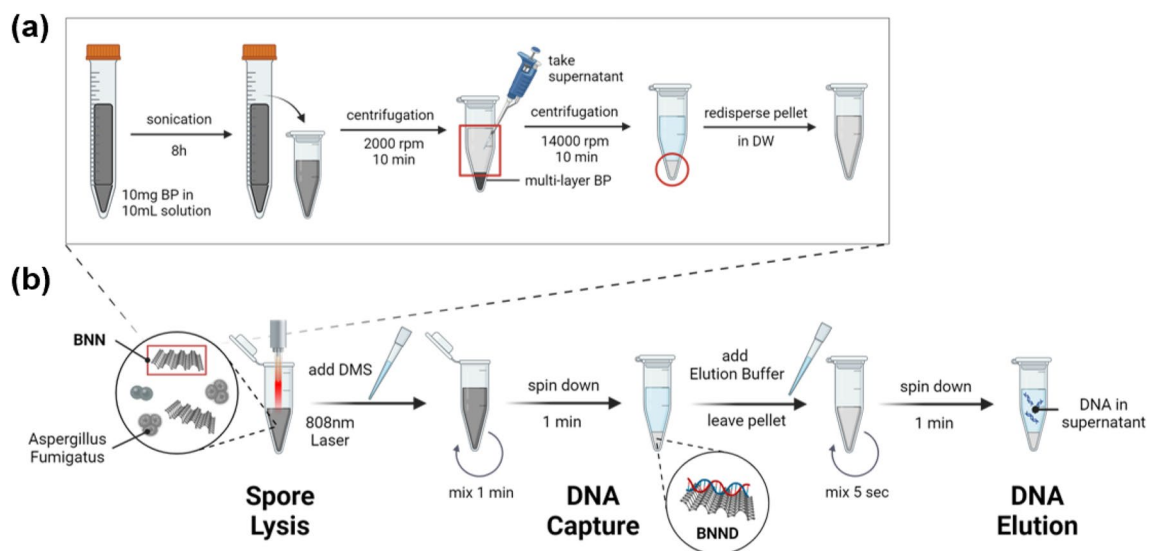


Fig. 1 Schematic Illustration of BNN-based fungal DNA extraction strategy. **a** The BNN-based DNA sample preparation strategy begins with the synthesis of monolayer BPNS materials through liquid-phase ultrasonic exfoliation and centrifugation. **b** The fungal

DNA-isolation assay, utilizing stabilized BNNs, consists of three stages: laser-irradiated BNNs functioning as the lysis buffer (spore lysis), DNA capture via the crosslinker DMS (DNA capture), and DNA elution as the final product (DNA elution)

Confocal microscopy (LSM 900, Carl Zeiss) and Fourier transform infrared spectroscopic (FT/IR-6300, Jasco Inc.) analysis of samples were also carried out to determine the mechanism of BNND-based fungal DNA extraction. For the confocal microscopy, 100 μL of 1 μM PI was treated to the spore pellets (pure spore, treated by laser, treated by BNN, treated by BNN under laser) and incubated in 37 $^{\circ}\text{C}$ for 30 min. Spores were centrifuged for 2 min, and their supernatant was removed. PI-treated spores were washed and resuspended in 1-mL PBS. 10 μL of spore solution was aliquoted on the slide glass and covered with cover glass, for confocal microscopy image.

2.6 *Aspergillus* Spore DNA Extraction Using BNNDs

Synthesized BNNs were used for the development and optimization of a BNND-based fungal DNA-isolation method, referring to the steps and mechanism of BP-NIR-HI System designed in the previous report [22]. The overall scheme of *Aspergillus* spore DNA-extraction protocol used in this study is shown in Fig. 1b. First, 200 μL of *Aspergillus* spore sample and 200 μL of BNN solution were added to a 1.5-mL centrifugation tube. Next, an 808 nm laser with a voltage of 4 A was applied to the solution from above for 5 min. Then, HI (DMS, 10 mg/mL) was added to the tube and thoroughly mixed for 1 min. After spinning down the tube for 1 min, the HI linkages between BNN and *Aspergillus* DNA create BNND composite, sinking down as the pellet, and the supernatant was discarded. Subsequently, pH 10.6 Elution Buffer was added to break the linkage and then the tube was gently vortexed for mixing. Herein, pH 10.6 Elution Buffer was prepared by adding a few drops of NaOH solution to a 20-mM Tris-HCl solution. Finally, *Aspergillus* spore DNA was eluted in the supernatant after spinning down for 1 min.

2.7 Fungal DNA Extraction Using Commercial Kit

The commercial QIAGEN QIAamp DNA Mini Kit was used to compare the efficiency of *Aspergillus* spore DNA isolation, as it showed high efficiency compared to other commercial fungal kits (Supplementary Figure S1). In the first step, 200 μL of *Aspergillus* spore sample, 200 μL of QIAGEN lysis buffer, and 20 μL of proteinase K were added to a 1.5-mL microcentrifuge tube. These components were mixed well by pulse-vortexing, and the solution was then incubated at 56 $^{\circ}\text{C}$ for 10 min. After incubation, 200 μL of 99% ethanol was added to the solution and gently mixed by pipetting. The mixture was then carefully transferred to the QIAamp Mini spin column and centrifuged at 8000 rpm for 1 min. Following this, the filtrate in the tube was discarded, and 500 μL of AW1 Buffer solution was added for washing, which was then centrifuged at 8000 rpm for 1 min. The resulting filtrate was again discarded and 500 μL of

AW2 Buffer solution was added. After centrifugation at 13,500 rpm for 3 min, the tube containing the resulting filtrate was discarded. Finally, the spin column was placed in a clean 1.5 mL microcentrifuge tube and 200- μL elution buffer was added on the column. DNA was eluted by the centrifugation at 8000 rpm for 1 min. The method introduced above is an in-house method, in which we modified the original protocol based on our available equipment and experimental purposes [34].

2.8 Real-time Quantitative Polymerase Chain Reaction (qPCR)

To evaluate the efficiency of fungal DNA isolation, real-time qPCR was conducted using the final isolated DNA. Quantitative PCR was performed using *AccuPower 2X GreenStar*TM qPCR Master Mix and specific primers designed using Primer Blast. Following specific primer sequences were used: forward (5- CAACCTCCCACCCGTGTCT -3) and reverse (5- CGCATTTTCGCTGCGTTCTT -3). The PCR reaction was conducted under the following conditions: initial denaturation step at 95 $^{\circ}\text{C}$ for 15 min, followed by 40 cycles of denaturation at 95 $^{\circ}\text{C}$ for 10 s, annealing at 60 $^{\circ}\text{C}$ for 20 s, and extension at 72 $^{\circ}\text{C}$ for 20 s, with a final elongation step at 95 $^{\circ}\text{C}$ for 10 s.

3 Results and Discussion

3.1 Principle of BNND-based Fungal DNA Extraction Method

Figure 1 illustrates the overall scheme of BNND assay for fungal DNA-isolation strategy. This BNND assay can enrich and extract fungal DNA in less than 15 min, with BNNs acting as the lysis buffer to break down spores and DMS serving as the cross-linking agent between BNNs and the released DNA. The sample preparation process begins with the synthesis of BNNDs (Fig. 1a). To produce mono-layer BP, liquid-phase ultrasonication and two-step centrifugation are used to separate it from multi-layer BP crystals. Fungal DNA can then be isolated using the synthesized BNND material, with the extraction technique divided into three steps as shown in Fig. 1b: breaking down the spore membrane utilizing the photothermal characteristics of BNN (Spore Lysis), creating BNND composite through linkage between BNN and released DNA via DMS (DNA Capture), and cutting the linkage for DNA isolation (DNA Elution). Compared to commercial kits, this BNND assay is neither labor-intensive nor time-consuming and does not require hazardous chemical reagents or heavy instruments. The photothermal characteristics of BNNs eliminate the need for a heat incubator for spore lysis, shortening the sample

preparation steps and preserving DNA integrity. Furthermore, BNNs are precisely exfoliated in organic solvents, increasing the stability and surface area of the material for effective implementation in the mechanism.

3.2 BPNSs Synthesized in Organic Solvents

The BNND method was developed using BPNS material synthesized through liquid-phase ultrasonic exfoliation. This method employs ultrasonic waves to disrupt the weak van der Waals interactions between layers of bulk BP, making the selection of a suitable solvent that does not impede this exfoliation process crucial [31]. Ideal solvents should be anhydrous and oxygen-free, as oxygenated water degrades BP, causing the layers to aggregate and reform into oxidized phosphorus compounds [27–29]. Therefore, in this study, four types of organic solvents (NMP, NaOH-saturated NMP (NMP–NaOH), IPA, and DMSO) were chosen for BPNS liquid exfoliation, with DW included for comparison. These solvents were selected based on their properties, which

provide low degradation rates and stable dispersions of phosphorene, resulting in a high yield of BP flakes through exfoliation [32, 33]. We compared the characterization of BPNSs synthesized in these different solvents to select the most efficient BPNS material for fungal DNA isolation.

Scanning electron microscopy (SEM) images of BPNS were obtained to compare the surface morphology of the materials (Fig. 2a, Supplementary Figure S2). While BPNS in DW showed high dispersity and large plane sizes, approximately ranging from 1 to 10 μm, BPNS synthesized in the four organic solvents exhibited a more uniform morphology with an average size of less than 4 μm, indicating the effective dispersal function of organic solvents in BPNS exfoliation, leading to more uniform BPNS with smaller thickness. BPNS in NMP–NaOH solvent (BNN) especially presented tiny and regular starburst structures with thin tubes extending from the center, showing that the addition of NaOH significantly affected the shape of the final product. DLS analysis in Fig. 2b, measured after two washes of the final BPNS product, indicated that the lateral dimensions

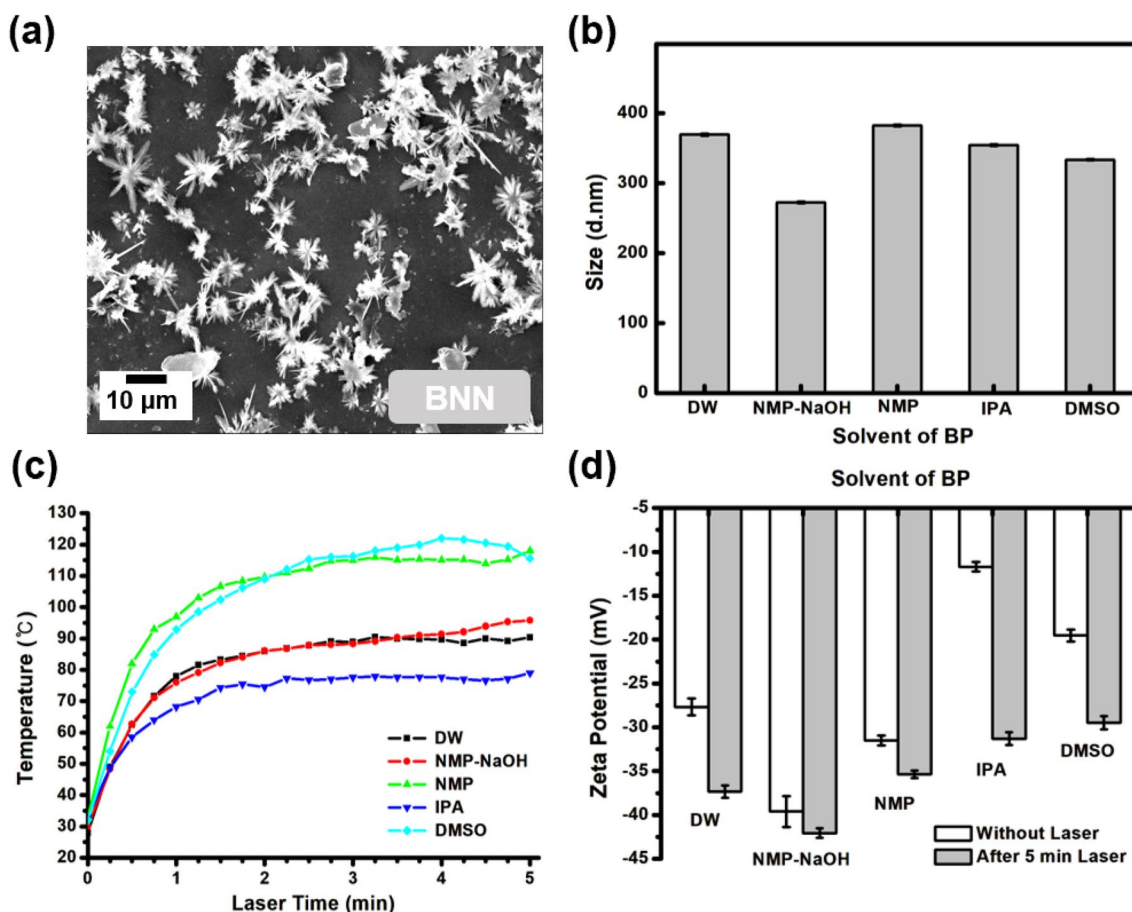


Fig. 2 Characterization of exfoliated BNND in organic solvents. **a** SEM image of BPNS synthesized in NMP–NaOH solvent (scale bars, 1 and 10 μm). **b** DLS results showing size differences of exfoliated BPNS in five types of solvents (DW, BNN, NMP, IPA, and DMSO).

c Temperature measurement during 5-min laser irradiation on exfoliated BPNS. **d** Zeta-potential values of exfoliated BPNS, measured under resting and photothermal conditions. Each test **b–d** was repeated three times

of the BP flakes align with the morphologic characteristics shown in SEM images. For the BPNS in NMP, the average hydrodynamic size was 382.3 nm (Z-average), with BPNS in DW at 369.1 nm, while BNN had sizes as thin as 272.3 nm. Although BNN exhibited starburst morphology, the flakes were uniformly dispersed in the solution, having a 2D size of 200–300 nm, representing an ideal expression of photothermal performance.

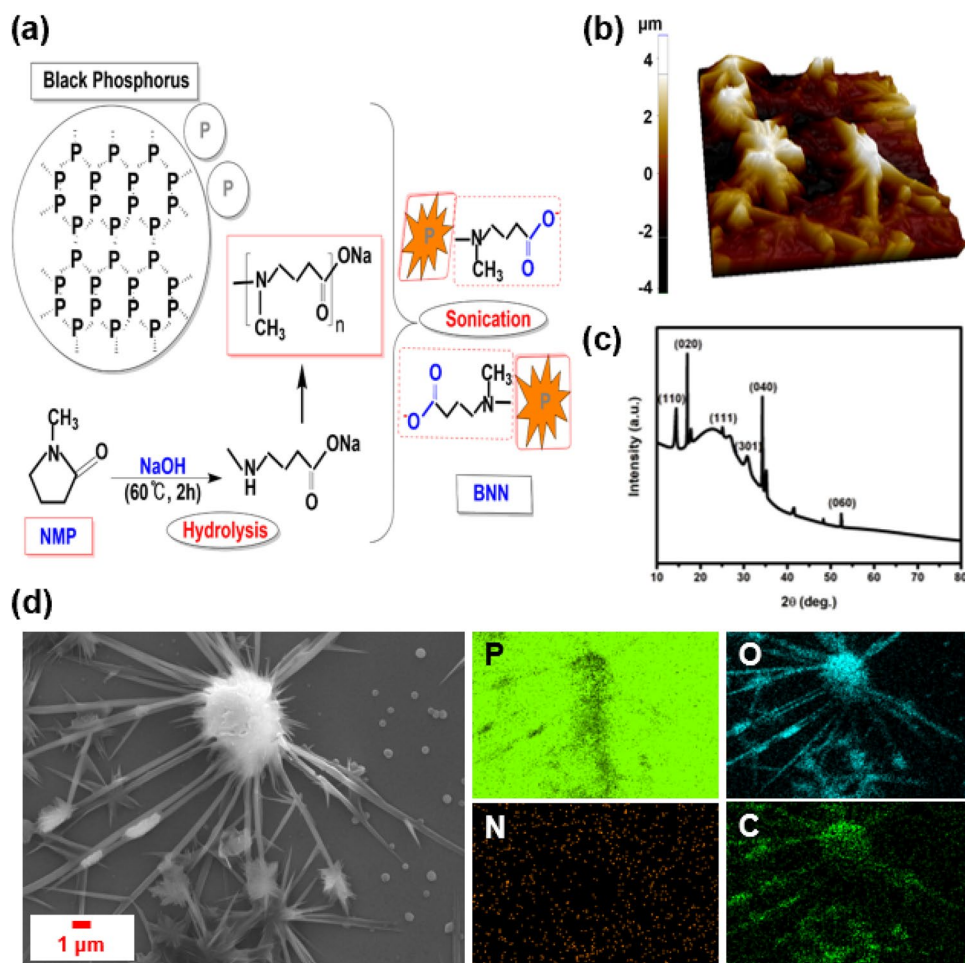
Furthermore, we investigated the photothermal characteristics of BNN by recording the temperature increase of the material after laser irradiation (Fig. 2c). Similar temperature growth trends were observed for BPNS in all solvent species with the same concentration. Notably, BNN exhibited a temperature rise of around 80 °C in 1 min and up to approximately 90 °C after 5 min of irradiation, a suitable temperature high enough to lyse the spore membrane but not too high to degrade DNA. Finally, we compared the surface charge of exfoliated materials in organic solvents under resting and photothermal conditions. The results indicated that light exposure did not affect the material's surface charge, but the increase in solution temperature due to photothermal effects moderately accelerated surface charge

movement (Fig. 2d). A zeta potential ranging from -40 to -45 mV indicated uniform dispersion and relative stability of BNN. In addition, the modest increase in surface charge under photothermal conditions suggested that BNN were relatively stable and easy to store. Taken together, these findings suggest that BNN holds promise for breakthroughs in material preservation and application.

3.3 Characterization of BNN Material

Through the analysis of BPNS materials, we identified that BNN demonstrated superior efficiency in all aspects of characterization. To further explore the structural aspects of BNN-assisted ultrasonic exfoliation, we investigated the potential chemical mechanisms involved. Given that NMP tends to decompose under alkaline conditions (approximately 50–70% decomposition in 4% sodium hydroxide over 8 h), it undergoes ring-opening to form sodium methyl-amino-butanoate [(CH₃)NH-CH₂-CH₂-CH₂-COONa]. This compound can polymerize, forming methyl-amino-butanoate end groups on the generated BNN and potentially acting as polymerization stoppers (Fig. 3a) [35]. This

Fig. 3 Characterization of BNN. **a** Schematic representation of NMP-hydrolysis reaction and synthesis of BNN through sonication. **b** AFM image of BNN, showing starburst-like surface structures. **c** XRD pattern of BNN for the analysis of crystal structures. **d** EDX results showing individual elemental maps (P, O, N, and C) of BNN



process may explain the formation of the starburst-like structure of BNN, as shown in Fig. 3b, where the flakes have a relative thickness of about 2 μm and a lateral size of around 10 μm . Moreover, no structural deformations were observed in this mechanically exfoliated sample, as evidenced by the absence of noticeable bubbles at the captured site. XRD data, collected over the 2θ range of 10° – 80° , were used to determine the crystal structure of BPNS material. XRD measurements of BPNS in DW, NMP, IPA, and DMSO showed strong intensities at the (020), (040), and (060) peaks, lacking other diffraction peaks, consistent with previously reported BP crystal patterns [36–38] (Supplementary Figure S3). However, the XRD pattern for BNN revealed additional diffraction peaks corresponding to the (110), (111), and (301) facets of exfoliated crystals, aligning with the starburst structure observed under electron microscopy AFM (Fig. 3c). Furthermore, the preferential growth of crystal facets and sharp diffraction peaks indicated a higher degree of crystallinity. We also verified and analyzed the elemental composition of the material using energy-dispersive X-ray spectroscopy (EDX) (Fig. 3d). EDX maps showed that, after ultrasonic exfoliation in the NMP–NaOH solvent, phosphorus (P) elements were uniformly distributed in the solution. The starburst-like structure was rich in carbon (C) and oxygen (O) elements, suggesting that hydrolyzed NMP had infiltrated and encapsulated the BPNS.

3.4 Mechanism of BNND Assay for Fungal DNA Extraction

Fungal spores exhibit strong environmental resilience, particularly in non-ideal extracellular conditions, where spore cell walls and membranes rapidly thicken to protect their internal structures from adverse conditions [39, 40]. Therefore, achieving rapid spore lysis through composite materials and technologies holds significant research importance for the molecular detection of spore DNA. Observation of untreated spore morphology via SEM and atomic force microscopy (AFM) revealed surface roughness and folds indicative of spore development stages, with naturally dehydrated cytoplasm forming concave wrinkles (Fig. 4a, Supplementary Figure S4a). When these spores were subjected to 808 nm laser irradiation, they exhibited a reduction in surface wrinkles and a transition to a thickened, rounded, and reinforced state (Fig. 4a), likely due to rapid immunostimulatory responses of the spores to the sudden laser environment. This indicates that laser irradiation not only facilitates spore lysis but also thickens cell walls and membranes, thereby complicating DNA release (Supplementary Figure S4a).

Treatment with BNN led to spore aggregation around BNN, possibly due to electrostatic attraction between BNN surface charges and spore surfaces, resulting in observed

spore rupture. Spores treated with BNN and subjected to 808-nm laser photothermal treatment demonstrated significant morphologic disruption and widespread fragmentation, suggesting enhanced spore-lysis properties through the BNN-laser composite system.

Several factors might contribute to the mechanism of spore lysis. First, the high temperature generated by BP irradiation, reaching around 100°C , denatures membrane proteins and releases intracellular organelles [41], leading to spore leakage. Second, reactive oxygen species (ROS) generated from BP nanosheets under heat stress induce spore lysis and cell apoptosis [22, 42, 43]. Furthermore, the starburst-like structures of BNN facilitate spore capture in the solution, aligning the photothermal effects of BNN and released ROS more closely with spores to achieve lysis (Supplementary Figure S5). In addition, the alkaline condition of NMP–NaOH solvent contributes to this process, as NaOH can dissolve alkaline-soluble parts of the outer cell wall, exposing inner hydrophobic proteins [44] and causing fungal spores to aggregate. Spore-viability test via confocal microscopy confirmed the membrane damage and DNA release from *Aspergillus* spores after BNN irradiation, showing increased propidium iodide fluorescence and the number of spore spots (Supplementary Figure S4b). This demonstrated that BNN serves as an effective lysis buffer in BNND-based fungal DNA extraction, successfully releasing *Aspergillus* DNA from the spores.

After spore lysis, the next step of the assay is to capture the released DNA effectively. We designed a BNN photothermal composite DMS crosslinking DNA extraction experimental scheme (Fig. 4b). We used a water-soluble and membrane-permeable homobifunctional imidoester crosslinker, DMS, due to its minimal cross-reactivity with nucleophilic groups in proteins, as previously reported [45–47]. The positive amine groups of DMS form linkages with the negative phosphate groups of dispersed *Aspergillus* DNA and the negatively charged carboxylate groups of BNN. This bridges the gap between BNN and freely dispersed DNA, aggregating the DNA on the BNN surface, which then sinks this BNND composite to the pellet after centrifugation. We conducted functional group detection on the DNA extraction using Fourier-transform infrared (FTIR) spectrum analysis to confirm that the linkage was well made. We observed characteristic functional groups of stable BNND obtained after hydrolysis and ultrasonic exfoliation of BNN, such as O–H at 3770 cm^{-1} , C–H at 2918 cm^{-1} , R–COO at 1636 cm^{-1} , N–H at 1051 cm^{-1} , and P–P ($815\sim 600\text{ cm}^{-1}$) (Figure S5a). In the BNND solution (Supplementary Figure S6b), we detected C=N at 2890 cm^{-1} , N–O at 1380 cm^{-1} , and N–C at 1200 cm^{-1} , providing strong evidence of BNND. However, when the DNA solution was added to BNN separately, no new composite bonds were detected (Supplementary Figure

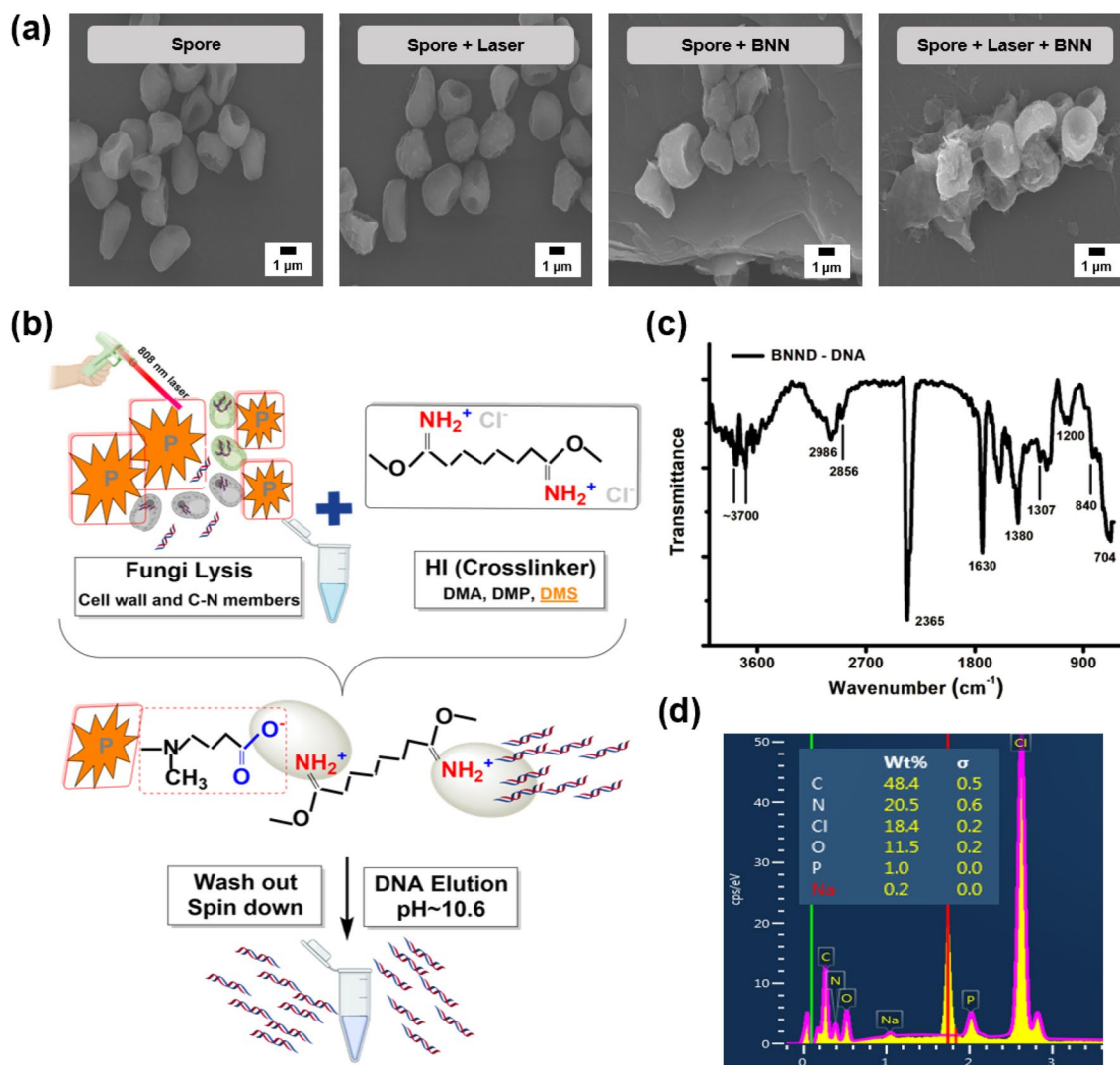


Fig. 4 Mechanism of BNND-based fungal DNA-isolation assay. **a** SEM images of *Aspergillus* spores under four different conditions (scale bar, 1 μm): untreated original spores, spores subjected to 808 nm laser irradiation for 5 min, spores mixed with BNN solution, and aggregated spores around BNND treated with 5-min laser

S6c). When BNND and DNA were combined, the high-frequency appearance of peaks at 1380 cm⁻¹, 1307 cm⁻¹, and 1200 cm⁻¹ indicated the formation of P-O bonds abundant in DNA and BNND (Fig. 4c). FTIR data analysis confirmed the applicability of the BNND assay for DNA binding and enrichment, with no significant attachment of protein bonds, thus preparing for relatively pure DNA elution. Elemental content was also confirmed through EDX experimental detection (Fig. 4d). The EDX spectrum of the aggregated pellet of DNA on the BNND surface showed five elements: C, N, Cl, O, and P. C, N, O, and P were from the released DNA; C, Cl, N, and O from DMS; and P from BP, confirming that the linkage between DNA and BNN had been well established.

irradiation. **b** Schematic explanation of DMS linkage between freely dispersed *Aspergillus* DNA and BNN. **c** FTIR results of the BNN, DMS, and *Aspergillus* DNA mixture. **d** EDX elemental spectrum of the BNN, DMS, and *Aspergillus* DNA mixture

3.5 Optimization and Applications of BNND-based Fungal DNA Extraction

Based on the material characterization and mechanism analysis conducted above, several optimization tests were carried out to determine the ideal conditions for fungal spore DNA isolation. To evaluate DNA-extraction efficiency, we varied one factor while keeping other experimental conditions constant as follows: 100 μL of *Aspergillus* spores of concentration 10⁶ spores per mL, 100 μL of BNN, 50 μL of 10 mg/mL DMS, 5-min irradiation with a 4A laser, and a pH 10.6 elution buffer. Real-time qPCR analysis of the final eluted DNA was performed, and Ct values were compared to assess the amount of DNA extracted under each specific

condition. Potential PCR inhibitors, including the effects of BPNS and DMS, were also considered beforehand to ensure accurate results. Experimental data showed that the small amounts of BP or DMS added barely exhibit any inhibition in PCR (Supplementary Figure S7a, b). Each optimization condition was repeated at least three times for verification.

The key mechanism of this BNND assay is the DMS linkage between BNN and freely dispersed DNA. Therefore, it is crucial to determine the appropriate ratio between these three materials. A too high concentration of either spores or BNN could hinder the linkage with DMS, whereas a concentration too low would reduce the likelihood of connection. Three candidate ratios between spores and BNN (1:1, 1:2, and 2:1) were tested for optimization, with 1:1 and 1:2 ratios showing the highest DNA elution (Fig. 5a). Five different concentrations of DMS were also tested, showing that concentrations as low as 5 mg/mL or as high as 100 mg/mL were not suitable (Fig. 5b). Furthermore, additional steps of the extraction protocol were optimized, including the time and current of laser irradiation, and the pH of the elution buffer. Analyzing the Ct values of each optimization test, laser irradiation for 5 min under 4 A showed relatively good efficiency (Supplementary Figure S7c, S7d) and a pH 10.5 elution buffer showed notable effectiveness in DNA

extraction compared to other pH conditions (Supplementary Figure S7e), which could be due to the DMS linkage being disrupted at pH 10.6. Through these optimization tests, experimental protocol conditions were established for further experiments, identified as white in the figures.

Following the optimized protocol, *Aspergillus* DNA spores (10^6 spores/mL) were extracted using BPNS synthesized in five different solvents (DW, NMP–NaOH, NMP, IPA, and DMSO) (Fig. 5c). Results demonstrated that *Aspergillus* DNA extraction using BPNSs displayed higher efficiency than using a commercial kit, regardless of the solvent used for BPNS synthesis. Among the five, the BNND assay showed a notably high rate of eluted DNA concentration, displaying around 3–5 threshold cycle (Ct) values lower than others. A Limit of Detection (LOD) test was also conducted to evaluate the potential for identifying pathogens at low concentrations (Fig. 5d). The results showed the lowest Ct values for the assay using BNN for every concentration of *Aspergillus* spores, from 10^8 to 10^1 spores per mL, compared to extraction using a kit or BPNS in DW. In addition, the isolation technique using BNN captured spores at concentrations as low as 10^1 spores in 1 mL, while the assay using the kit detected down to 10^3 spores per mL and BPNS in DW to 10^2 spores per mL. Therefore, the detection technique using

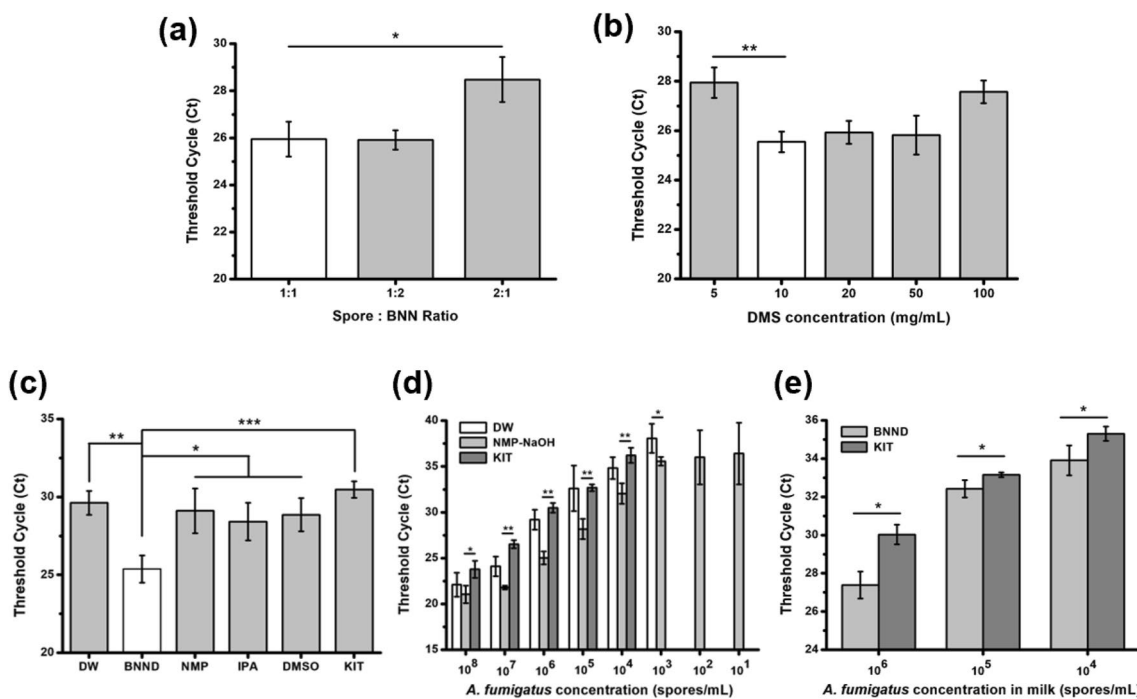


Fig. 5 Optimization and applications of BNND assay for fungal DNA extraction. **a** qPCR results of the optimization test on the ratio of *Aspergillus* spores to BNN volume. **b** qPCR results of the optimization test on DMS concentration (mg/mL). **c** qPCR results of DNA extraction from *A. Fumigatus* spores (10^6 per mL) using BPNSs exfoliated in five different solvents or a commercial kit. **d** Limit of Detection (LOD) test of *Aspergillus* DNA isolation from 10^8 to 10^1 spores per mL, using a commercial kit, BPNS in DW, and BNND. **e** Detection of *Aspergillus* in contaminated milk. Each test **a–e** was repeated three times. The statistical significance of the differences was evaluated using Student’s *t*-test. The levels of significance used are as follows: * $p < 0.05$; ** $p < 0.01$; *** $p < 0.001$

tion (LOD) test of *Aspergillus* DNA isolation from 10^8 to 10^1 spores per mL, using a commercial kit, BPNS in DW, and BNND. **e** Detection of *Aspergillus* in contaminated milk. Each test **a–e** was repeated three times. The statistical significance of the differences was evaluated using Student’s *t*-test. The levels of significance used are as follows: * $p < 0.05$; ** $p < 0.01$; *** $p < 0.001$

BNND demonstrated sensitivity in capturing low amounts of fungal DNA and efficiency in eluting the captured DNA, showing potential for clinical applications where early diagnosis of disease is crucial.

Another possible application of this BNND-based fungal DNA-extraction method is in the field of food chemistry. *Aspergillus* species are known to contaminate food or drink substrates, producing mycotoxins that are harmful to health when consumed [48]. Therefore, rapid and accurate detection of *Aspergillus* in spoiled food is a significant issue to address. The potential and efficiency of *Aspergillus* detection using our method were also investigated with milk contaminated with *Aspergillus fumigatus* (Fig. 5e). Repetition of experiments with *Aspergillus* concentrations of 10^6 and 10^4 spores per mL in milk displayed more efficient results with our BNND-based isolation method compared to the protocol using a commercial kit. These findings open possibilities and prospects for our BNND-based fungal DNA-isolation method to be applied in diverse research fields, including medical diagnostics, food and environmental science.

4 Conclusion

The present study developed and optimized a fungal DNA-extraction technique utilizing stabilized BNNs. BPNs synthesized in organic solvent, especially in NMP–NaOH, provided increased stability and better performance in DNA-isolation mechanism. By harnessing the photothermal effects of BNNs, we sought to achieve spore lysis up to cell wall, without the need of extra incubation steps nor harsh chemical agents, thereby preserving DNA purity and integrity. Linkage with DMS was also enhanced through increased surface area of BNNDs, improving the overall DNA-elution quantity and extraction efficiency. The novel BNND-based fungal DNA-isolation strategy, as illustrated in Fig. 1, can enrich and extract fungal DNA in under 15 min. BNNs serve as the lysis buffer to break down spores, while DMS acts as the cross-linking agent between BNNs and released DNA. The process begins with BNN synthesis using liquid-phase ultrasonication and two-step centrifugation to produce mono-layer BP. The isolation technique involves three steps: spore membrane breakdown (Spore Lysis), DNA linkage creation (DNA Capture), and DNA isolation (DNA Elution). The findings propose a new DNA-extraction method, utilizing stabilized BNNDs, which can rapidly and effectively isolate fungal DNA with high sensitivity and specificity, demonstrating promising applications in diagnostics and beyond. Nevertheless, further study with more validation data on clinical samples and drink tests would be needed for real-life applications on fungal DNA extraction in medical and environmental science fields. These results overall

underscore the innovative potential of BNND method for DNA-extraction method across various areas. Overall, the BNND-based strategy provides simple and rapid protocol with increased efficiency in fungal DNA isolation, exhibiting potential across diverse fields, especially in clinical applications.

Supplementary Information The online version contains supplementary material available at <https://doi.org/10.1007/s13206-024-00173-z>.

Author contributions S.M.L. and H.L. contributed equally to this work. Y.S. supervised the project. Y.S., S.M.L., and H.L. conceived the research, designed the experiments, and performed the analysis and made interpretations of the data. E.Y.L., M.G.K., H.J.L., Y.R., M.L., and B.K. provided chemicals and supported the data analysis. Y.S., S.M.L., and H.L. wrote and edited the manuscript. All authors read and approved the final manuscript.

Funding This study was supported by the Ministry of Science, ICT and Future Planning (MSIP) through the National Research Foundation of Korea (NRF) (2020R1A2C2007148), Republic of Korea.

Declarations

Conflict of interest The authors declare no conflicts of interest.

References

- Liu, Q., et al.: Advances in the application of molecular diagnostic techniques for the detection of infectious disease pathogens. *Mol. Med. Rep.* **27**, 1–14 (2023)
- Chen, F., et al.: Multiplex detection of infectious diseases on microfluidic platforms. *Biosensors* **13**, 410 (2023)
- Paterson, R.R.M., Solaiman, Z., Santamaria, O.: Guest edited collection: fungal evolution and diversity. *Sci. Rep.* **13**, 21438 (2023)
- Rokas, A.: Evolution of the human pathogenic lifestyle in fungi. *Nat. Microbiol.* **7**, 607–619 (2022)
- Fang, W., et al.: Diagnosis of invasive fungal infections: challenges and recent developments. *J. Biomed. Sci.* **30**, 42 (2023)
- AlMaghrabi, R.S., et al.: Challenges in the management of invasive fungal infections in the Middle East: expert opinion to optimize management using a multidisciplinary approach. *Cureus* (2023). <https://doi.org/10.7759/cureus.44356>
- Hussain, K., et al.: Biosensors and diagnostics for fungal detection. *J. Fungi* **6**, 349 (2020)
- Malhotra, S., et al.: Recent diagnostic techniques in mycology. *J. Med. Microbiol. Diagn.* (2014). <https://doi.org/10.4172/2161-0703.1000146>
- Vijayarajan, R.S., Pushpanathan, P.: Fungal infections: advances in diagnosis and treatment. In: *Fungi bio-prospects in sustainable agriculture, environment and nano-technology*, pp. 515–539. Elsevier, Amsterdam (2021)
- Khot, P.D., Fredricks, D.N.: PCR-based diagnosis of human fungal infections. *Expert Rev. Anti Infect. Ther.* **7**, 1201–1221 (2009)
- Griffiths, L.J., et al.: Comparison of DNA extraction methods for *Aspergillus fumigatus* using real-time PCR. *J. Med. Microbiol.* **55**, 1187–1191 (2006)
- Riffiani, R., Wada, T., Shimomura, N., Yamaguchi, T., Aimi, T.: An optimized method for high-quality DNA extraction medicinal fungi *Mycocleptodonoides aitchisonii* for whole genome sequencing. *IOP Conf Ser Earth Environ Sci* **948**, 012032 (2021)

13. Hoorzook, K.B., Barnard, T.G.: Comparison of DNA extraction methods for the direct quantification of bacteria from water using quantitative real-time PCR. *Water* **14**, 3736 (2022)
14. Dairawan, M., Shetty, P.J.: The evolution of DNA extraction methods. *Am. J. Biomed. Sci. Res* **8**, 39–45 (2020)
15. Uda, M.A., et al.: Evaluation and optimization of genomic DNA extraction from food sample for microfluidic purpose. *IOP Conf Ser Mater Sci Eng* **743**, 012031 (2020)
16. Galliano, I., et al.: Comparison of methods for isolating fungal DNA. *Pract. Lab. Med.* **25**, e00221 (2021)
17. Saitoh, K.-I., Togashi, K., Arie, T., Teraoka, T.: A simple method for a mini-preparation of fungal DNA. *J. Gen. Plant Pathol.* **72**, 348–350 (2006)
18. Cheng, X., Chen, G., Rodriguez, W.R.: Micro-and nanotechnology for viral detection. *Anal. Bioanal. Chem.* **393**, 487–501 (2009)
19. Qiao, Z., et al.: A simple and rapid fungal DNA isolation assay based on ZnO nanoparticles for the diagnosis of invasive aspergillosis. *Micromachines* **11**, 515 (2020)
20. Qiao, Z., et al.: Simple and sensitive diagnosis of invasive aspergillosis using triphasic DE–ZnO–APDMS microparticle composite. *Sens. Actuators B Chem.* **346**, 130487 (2021)
21. Liu, H., et al.: Large instrument-and detergent-free assay for ultra-sensitive nucleic acids isolation via binary nanomaterial. *Anal. Chem.* **90**, 5108–5115 (2018)
22. Liu, H., et al.: Homobifunctional Imidoester combined black phosphorus nanosheets used as cofactors for nucleic acid extraction. *BioChip J.* **16**, 58–66 (2022)
23. Cheng, J., et al.: Two-dimensional black phosphorus nanomaterials: emerging advances in electrochemical energy storage science. *Nano-Micro Lett.* **12**, 1–34 (2020)
24. Ding, J., Qu, G., Chu, P.K., Yu, X.F.: Black phosphorus: versatile two-dimensional materials in cancer therapies. *View* **2**, 20200043 (2021)
25. Xie, Z., et al.: Black phosphorus-based photothermal therapy with aCD47-mediated immune checkpoint blockade for enhanced cancer immunotherapy. *Light Sci. Appl.* **9**, 161 (2020)
26. Liu, H., et al.: Black phosphorus, an emerging versatile nanoplatform for cancer immunotherapy. *Pharmaceutics* **13**, 1344 (2021)
27. Wood, J.D., et al.: Effective passivation of exfoliated black phosphorus transistors against ambient degradation. *Nano Lett.* **14**, 6964–6970 (2014)
28. Liu, X., Wood, J.D., Chen, K.-S., Cho, E., Hersam, M.C.: In situ thermal decomposition of exfoliated two-dimensional black phosphorus. *J. Phys. Chem. Lett.* **6**, 773–778 (2015)
29. Huang, Y., et al.: Interaction of black phosphorus with oxygen and water. *Chem. Mater.* **28**, 8330–8339 (2016)
30. Huang, X., et al.: Multifunctional layered black phosphorene-based nanoplatform for disease diagnosis and treatment: a review. *Front. Optoelectron.* **13**, 327–351 (2020)
31. Ge, X., Xia, Z., Guo, S.: Recent advances on black phosphorus for biomedicine and biosensing. *Adv. Func. Mater.* **29**, 1900318 (2019)
32. Rabiei Baboukani, A., Khakpour, I., Drozd, V., Wang, C.: Liquid-based exfoliation of black phosphorus into phosphorene and its application for energy storage devices. *Small Struct.* **2**, 2000148 (2021)
33. Lin, S., Chui, Y., Li, Y., Lau, S.P.: Liquid-phase exfoliation of black phosphorus and its applications. *FlatChem* **2**, 15–37 (2017)
34. Löffler, J., Hebert, H., Schumacher, U., Reitze, H., Einsele, H.: Extraction of fungal DNA from cultures and blood using the QIAamp Tissue Kit. *Qiagen News* **4**, 16–17 (1996)
35. Ou, Y.J., Wang, X.M., Li, C.L., Zhu, Y.L., Li, X.L.: The effects of alkali and temperature on the hydrolysis rate of N-methylpyrrolidone. *IOP Conf. Ser. Earth Environ. Sci.* **100**, 012036 (2017)
36. Sarswat, P.K., Sarkar, S., Cho, J., Bhattacharyya, D., Free, M.L.: Structural and electrical irregularities caused by selected dopants in black-phosphorus. *ECS J. Solid State Sci. Technol.* **5**, Q3026 (2016)
37. Mayorga-Martinez, C.C., et al.: Metallic impurities in black phosphorus nanoflakes prepared by different synthetic routes. *Nanoscale* **10**, 1540–1546 (2018)
38. Flores, E., et al.: Thermoelectric power of bulk black-phosphorus. *Appl. Phys. Lett.* (2015). <https://doi.org/10.1063/1.4905636>
39. Bauda, E., et al.: Ultrastructure of macromolecular assemblies contributing to bacterial spore resistance revealed by in situ cryo-electron tomography. *Nat. Commun.* **15**, 1376 (2024)
40. Setlow, P., Christie, G.: New thoughts on an old topic: secrets of bacterial spore resistance slowly being revealed. *Microbiol Mol Biol Rev* **87**, e00080–e122 (2023)
41. Shehadul Islam, M., Aryasomayajula, A., Selvaganapathy, P.R.: A review on macroscale and microscale cell lysis methods. *Micromachines* **8**, 83 (2017)
42. Noor, R.: Mechanism to control the cell lysis and the cell survival strategy in stationary phase under heat stress. *Springerplus* **4**, 1–9 (2015)
43. Luo, M., Fan, T., Zhou, Y., Zhang, H., Mei, L.: 2D black phosphorus-based biomedical applications. *Adv. Func. Mater.* **29**, 1808306 (2019)
44. Zhang, H., et al.: The aggregation of *Aspergillus* spores and the impact on their inactivation by chlorine-based disinfectants. *Water Res.* **204**, 117629 (2021)
45. Liu, H., et al.: A sample preparation technique using biocompatible composites for biomedical applications. *Molecules* **24**, 1321 (2019)
46. Liu, H., et al.: Facile homobifunctional imidoester modification of advanced nanomaterials for enhanced antibiotic synergistic effect. *ACS Appl. Mater. Interfaces* **13**, 40401–40414 (2021)
47. Koo, B., et al.: A novel platform using homobifunctional hydrazide for enrichment and isolation of urinary circulating RNAs. *Bioeng. Transl. Med.* **8**, e10348 (2023)
48. Navale, V., Vamkudoth, K.R., Ajmera, S., Dhuri, V.: *Aspergillus* derived mycotoxins in food and the environment: Prevalence, detection, and toxicity. *Toxicol. Rep.* **8**, 1008–1030 (2021)

Publisher's Note Springer Nature remains neutral with regard to jurisdictional claims in published maps and institutional affiliations.

Springer Nature or its licensor (e.g. a society or other partner) holds exclusive rights to this article under a publishing agreement with the author(s) or other rightsholder(s); author self-archiving of the accepted manuscript version of this article is solely governed by the terms of such publishing agreement and applicable law.